UAV IMAGES HAVING JOINT COLOUR AND SHAPE FEATURE TO DETECT EARTHQUAKE TRIGGERED ROOF HOLES

[1]AFRA FATIMA, [2] G. ARUNA, [3] K. PREMLATHA.
[1]PG Scholar, Dept of DSCE, Shadan Women's College of Engineering and Technology, Hyderabad, TS, India.
[2]Assoc Professor, Dept. of ECE, Shadan Women's College of Engineering and Technology, Hyderabad, TS, India.
[3]Assoc Professor, Dept. of ECE, Shadan Women's College of Engineering and Technology, Hyderabad, TS, India.

Abstract: Numerous strategies have been produced to distinguish harmed structures because of tremor. Notwithstanding, little consideration has been paid to examine somewhat influenced structures. In this letter, an unsupervised strategy is exhibited to know seismic tremor activated "rooftop openings" on rustic houses from unmanned airborne vehicle (UAV) pictures. To begin with, both orthovariety and inclination pictures are created from an organization of UAV pictures. At that point, an adjusted Chinese eatery establishment display is utilized to take in an unsupervised model of the geo-protest classes in the zone by intertwining both over portioned orthovariety and angle pictures. At long last, "rooftop gaps" on country houses are distinguished utilizing the educated model.

Keywords: Unmanned Airborne Vehicle (UAV) Pictures.

I. INTRODUCTION

Seismic tremor activated building harm and even fall is a noteworthy reason of mortality. The sum and grade of harm are basic data in a fiasco regions, and it focuses on the significance of a fast and solid location of harmed zones, particularly in the periods of safeguard and recuperation. With the advancement of spatial data innovation, remote detecting symbolism has turned into an essential information source to distinguish and survey harmed or fallen structures in hard hit regions. As of late, numerous investigations utilizing space and flying pictures to recognize quake actuated building harm or crumple have been finished on account of their high spatial determination and generally ease. For the most part, four sorts of procedures have been utilized to identify harmed or crumbled structures because of seismic tremor.

1) The first is visual translation. For the most part, great consequences of harm recognition can be acquired by visual translation in these examinations. In any case, the time has come expending, requires talented specialists, and prompts an overwhelming work.

2) The second technique takes present arrangement examination on recognize building harm. As contrasted and the outcomes from the pixel-based technique, protest based strategies are less influenced by the purported "salt and pepper" issue The primary favorable position of these kinds of strategies is programmed task. In any case, the underlying characterization result has awesome impact to the last building harm identification.

3) Third one is to distinguish the fell structures by utilizing the contrast amongst pre-and posts seismic advanced surface models (DSMs). DSMs made from pre-and post-seismic stereo photos to identify the structures which have fell by a tremor.

4) The fourth is to ascertain the stature of the crumbled structures utilizing building shadows. The reason for this letter is to exhibit an unsupervised technique to distinguish seismic tremor activated "rooftop gaps" on provincial houses.

There are three stages of the proposed strategy. To start with, both orthomosaic and inclination pictures are produced from an arrangement of post seismic unmanned flying vehicle (UAV) pictures. At that point, an altered Chinese eatery establishment (CRF) display is utilized to take in an unsupervised model of the geo-question classes in the influenced region. In particular, the scholarly model wires both the over fragmented orthomosaic and inclination pictures. At long last, the "rooftop openings" are distinguished utilizing the scholarly model. However, little attention has been paid to analyze slightly affected buildings (e.g., Grade 2 or Grade 3 in EMS98 [16]). The purpose of this letter is to present an unsupervised method to detect earthquake-triggered "roof-holes" on rural houses. There are three steps of the proposed method. First, both orthomosaic and gradient images are generated from a set of post-seismic unmanned aerial vehicle (UAV) images. Then, a modified Chinese restaurant franchise (CRF) model is employed to learn an unsupervised model of the geo-object classes in the affected area. Specifically, the learned model fuses both the over segmented orthomosaic and gradient images. Finally, the "roof-holes" are detected using the learned model. The proposed method is confirmed by using post event UAV images from the 2013 Ya'an earthquake, and the performance is evaluated in view of both qualitative and quantitative measurements.

II. METHODOLOGY

In this section, the proposed method for detecting roof-holes is presented in detail. The flowchart of the proposed method is shown in Fig. 2, which consists of three sequent steps: 1) the orthomosaic image and gradient image of the study area are derived from the UAV images; 2) the two images are fused using the CRF model to obtain a clustering result; and 3) the roof-holes are detected from this clustering result.

III. EXISTING SYSTEM

A nitty gritty examination of the attributes of the zones harmed because of the Bam tremor as far as the distinctions in the backscattering coefficient and the connection coefficient of the pre-and post-occasion Envisat/ASAR pictures was led keeping at the top of the priority list the true objective to raise the exactness of harm recognition. At long last, the harm mapping plan was reconsidered to exhibit the appropriation of harmed regions in Bam. The backscattered quality of microwaves mirrors the unpleasantness of the surface, the dampness level, and the occurrence edge of the microwaves and its wavelength. Ordinarily, man-influenced structures to demonstrate generally high reflections because of phantom qualities called the "cardinal impact of

structures and ground." Open spaces or harmed structures have moderately low reflectances, since microwaves are scattered in various ways. In view of the above attributes, the creators already built up a computerized strategy for distinguishing regions with seriously harmed structures utilizing the time arrangement SAR informational indexes for the Kobe seismic tremor _Matsuoka and Yamazaki 2004_. This experimental technique is portrayed in the following passage.

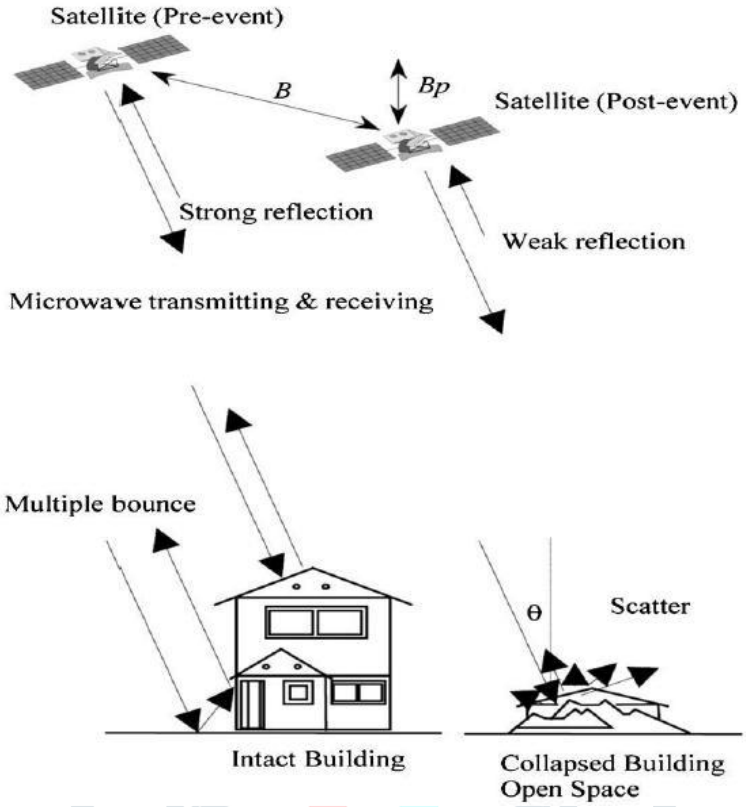

Initial, two multi-looked force pictures taken when a quake were readied. It is alluring that the procurement dates are as close as conceivable to the day of the tremor and that the perception conditions are comparable. In any case, the strategy was fruitful in harm location for the Kobe case, in resentment of the way that the picture match had inconceivably extraordinary perception circles when the tremor. After co-enlisting the pre-and post-occasion pictures, each picture was separated utilizing a Lee channel with a 21*21 pixel window. The average circumstance was seen in the backscattering attributes in the territory with various fallen structures in downtown Bam. demonstrate the pre-and post-seismic tremor pictures of the zone by QuickBird and Envisat, individually. The backscattered echoes by extremely harmed regions diminished in the post-picture of Envisat. In any case, it likewise found that a turnaround trademark overwhelmed in some extremely harmed zones in southeastern Bam. Preceding the seismic tremor, systematic houses with level rooftops were thickly found, yet the quake harmed a large portion of them. As indicated by the Envisat pictures, the backscattered echoes ended up more grounded in the post quake picture.
The flotsam and jetsam from the crumbled structures could likewise make a moderately higher reflectance of microwaves than smooth/level rooftop surfaces. Keeping at the top of the priority list the true objective to reconsider the model in view of the above experience, a more careful examination of the backscattering qualities in the harmed and non-harmed regions.

IV. PROPOSED SYSTEM

A. Data Preprocessing

In this section, the postseismic UAV images are processed in order to get the orthomosaic image and the gradient image which are required as the input for the CRF model in the next step.

1) Orthomosaic Image: The postseismic UAV images are processed with the Pix4UAV software [15]. After that, we derived two types of data of the study area: the orthomosaic image with the size of 5000 ⨯ 5000 pixels and 3-D point clouds with the average point density of 403 points/m2.

2) Gradient Image: The 3-D point clouds reconstructed from the UAV images are endowed with three visible bands, and the point spacing in the 3-D point clouds is approximately 15 cm. In order to employ the shape feature of point clouds, they need to be further processed. First, the original point clouds were transferred to DSM [Fig. 3(a)] in ENVI IDL and filtered to extracted terrain XYZ points using morphological filter. This terrain points were further processed in ArcMap to generate DEM [Fig. 3(b)], and both DSM and DEM were resampled to the same resolution of orthomosaic image. Then, the normalized DSM (nDSM) [Fig. 3(c)] was generated by subtracting the DEM from the DSM, which only represents the nonterrain objects. The primary advantage of the nDSM is that it removes the effect of undulation of topography in the mountain area. Finally, a gradient image [Fig. 3(d)] was generated from the nDSM using the algorithm [17].

According to the experiments, it is concluded that the number of clusters for the gradient image is set to three. For each class, we counted the frequencies of pixels on each gradient value. As shown in Fig. 4, most pixels in class 1 have a lower gradient value, which indicates the houses with flat roofs; the pixels in class 3 have a much higher gradient value, which refers to the boundary of houses. It is worth mentioning that the gradient value of most pixels in class 2 is slightly higher than that of class 1, which indicates the houses with pitched roofs. Since most of the roof-holes occurred in the pitched roofs, the pixels in class 2 include the “roof-holes.”

B. CRF With Joint Color and Shape Features

In this section, a modified CRF model, which could fuse color and shape features, is introduced to detect earthquake triggered roof-holes. The CRF is a construction method on the hierarchical Dirichlet process. In the CRF metaphor, suppose that a customer enters a restaurant, and the customer randomly chooses to either sit at an existing table or start a new table; customers who sat at a table randomly select a dish to eat. More details on table selection and dish selection in CRF can be found in [18]. Initially, the CRF model is a clustering model, which is applied in information retrieval and text modeling. In this letter, in order to describe the clustering problem using UAV images with joint color and shape feature, an improved CRF model is employed to detect the earthquake-triggered roof-holes. The procedure of the proposed model is shown in Fig. 5. In the proposed model, there are two types of observation data, i.e., an orthomosaic image *XO* with color feature [Fig. 5(b1)] and a gradient image *XG* with shape feature [Fig. 5(b2)] of the same geographic location. The two observations are separated into *L* over segmentations using the algorithm [19]. In the proposed model, the "restaurant" is defined as a squared area which contains some neighborhood over segmentations as shown in Fig. 5(c). The "customer θ" is associated with an over segmentation, and each customer is described by two feature vectors, i.e., shape and color features.

C. Roof-Hole Detection

In this section, the goal is to find "roof-hole" segments (i.e., over segmentations) from the clustering result. In this case, it is done by comparing the distribution of each segment in the clustering result and distribution of "roof-hole" segments in the ground truth. The similarity between two distributions is calculated based on Kullback–Leibler (KL) divergence. For each "roof-hole" segment in the ground truth, all of the segments in the clustering result can be sorted according to their scores computed by KL divergence. Then, the most representative segments with high scores can be selected as the detected roof-holes.

V. EXPERIMENTAL RESULTS AND DISCUSSIONS

In this section, the performance of the proposed method for detecting roof-holes is evaluated. First, the number of clusters for the data set is selected. Then, the performance of the proposed method is evaluated in terms of both qualitative and quantitative aspects.

A. Model Parameter

In the proposed method, the number of clusters for the orthomosaic image and gradient image needs to be given in advance. First, based on the experiments and analysis of the gradient image, the number of clusters for the gradient image is set to 3. Second, the minimum description length criterion [20]–[23] is employed to select the optimal number of clusters for the orthomosaic image, and number 12 is selected as the optimal number of clusters.

B. Evaluation of the Results

In this section, the performance of the proposed method is compared with K-means and ISODATA algorithms, from the viewpoint of both qualitative and quantitative aspects. The input of K-means and ISODATA is the orthomosaic image, and the number of clusters is set to 12. Furthermore, in order to compare with the proposed method, the "roof-hole" class of two reference algorithms is extracted from their clustering results by visual inspection.

1) ***Qualitative Evaluation****:* As shown in Fig. 6, there are at least two important differences between the detection results using the proposed method and two reference algorithms.

a) Cluster label for the roof-holes: In both K-means and ISODATA algorithms, the clustering results are guided with only spectral information. Since roof-holes and shadows have high similarity of the spectral properties, most of the roof-holes are confused with the building shadows. However, the proposed method can distinguish the roof-holes from the shadows. Although roof-holes and shadows have higher similarity in spectra, they are different in shape feature. Therefore, the shape is a very important cue to make a distinction between roof-holes and shadows in the proposed method.

b) Object-oriented feature of the results: Compared with the results of both K-means and ISODATA, the detection result of the proposed method seems to be more compact. In other words, the result of the proposed method seems to have object-oriented property. Specifically, an individual pixel is taken as a sample in both K-means and ISODATA. However, a group of neighbor pixels called an over segmentation in this letter is regarded as a sample in the proposed method, where the label for a pixel is inferred through all related pixels using joint color and shape features.

2) ***Quantitative Evaluation****:* The main aim of object detection is to assign labels to each pixel of the image. In this letter, the only object that we are concerned is the roof-holes, and so, there are only two class labels, i.e., "roof-holes" and "background," for all pixels in the image. For K-means and ISODATA, the "roof-hole" cluster is extracted from their clustering results by visual interpretation, and other clusters belong to "background." Thus, the accuracy evaluation of the roof-hole detection is based on four statistics, which are the following: true positive (TP), false positive (FP), true negative (TN), and false negative (FN).

In this case, we utilize four indices to describe the performance of an algorithm, which are *accuracy*, *sensitivity*, false negative ratio (FNR), and false positive ratio (FPR) [24]. The four indices are computed as follows:

$$Accuracy = \frac{(TP + TN)}{(TP + TN + FP + FN)}$$

$$Sensitivity = \frac{TP}{(TP + FN)}$$

$$FNR = \frac{FN}{GT}$$

$$FPR = \frac{FP}{GT}$$

Where GT refers to the "roof-holes" in the ground truth. *Accuracy* indicates the proportion of correctly detected "roof-holes" and "background" in the whole data. *Sensitivity* represents the proportion of correctly detected "roof-holes" in all detected "roof-holes." In addition, FNR is the proportion of "roof-hole" commission errors in GT of the ground truth, and FPR is the proportion of "roof-hole" omission error in GT of the ground truth.

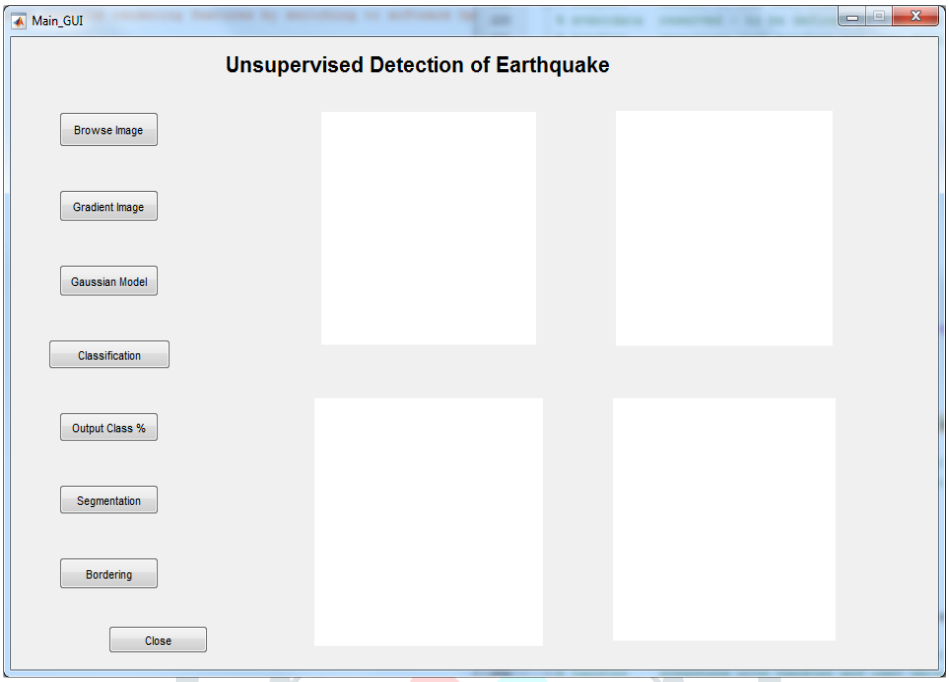

Green Channel Image

Blue Channel Image

Gradient Magnitude

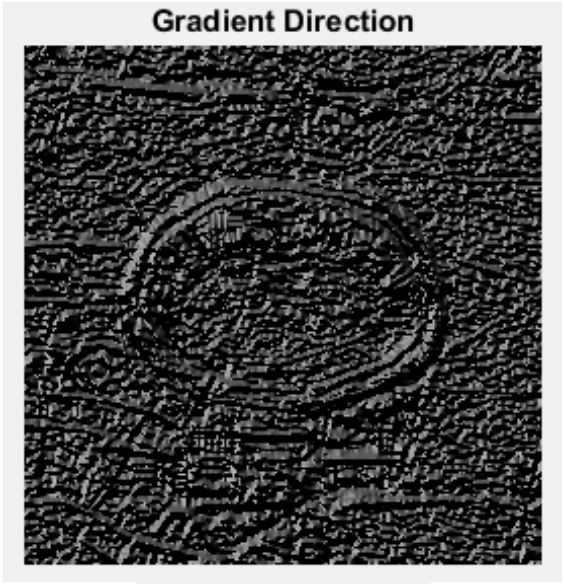


```
Percentage of Water :
     0

Percentage of Urban Area :
   10.0540

Percentage of Crop_1 :
   74.8230

Percentage of Crop_2 :
    0.6241

Percentage of Vegetation :
   14.4989
```

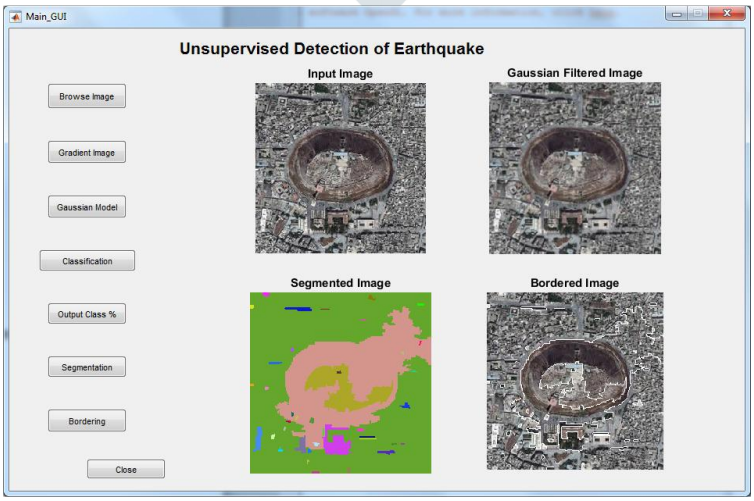

VI. CONCLUSION

In this letter, an unsupervised technique has been introduced to know tremor instigated rooftop openings utilizing UAV pictures with joint shading and figure highlights, and the exploratory outcomes are tasteful. Be that as it may, the planned technique has one restriction: it may not perform so well in the houses with level rooftops. It is on the grounds that the structure of the houses with level rooftops is steel solid structure and its hostile to seismic execution is more grounded; a couple of rooftop gaps happened in the houses with level rooftops. By and large, recognizable proof of somewhat influenced houses remains a test, even with 0.5-m determination remote detecting information. Luckily, this application, identifying seismic tremor actuated "rooftop openings" utilizing UAV pictures, was attempted in this letter, and the outcomes are extremely reassuring. The UAV pictures with 3-D point mists, as one of the integral information, give a conceivable answer for identify the somewhat influenced houses.

VII. REFERENCES

[1] M. Matsuoka and F. Yamazaki, "Building damage mapping of the 2003 Bam, Iran, earthquake using Envisat/ASAR intensity imagery," *Earthquake Spectra*, vol. 21, no. S1, pp. 285–294, Dec. 2005.

[2] L. Dong and J. Shan, "A comprehensive review of earthquake-induced building damage detection with remote sensing techniques," *ISPRS J. Photogramm. Remote Sens.*, vol. 84, pp. 85–99, Oct. 2013.

[3] P. Gamba, F. D. Acqua, and G. Trianni, "Rapid damage detection in Bam area using multitemporal SAR and exploiting ancillary data," *IEEE Trans. Geosci. Remote Sens.*, vol. 45, no. 6, pp. 1582–1589, Jun. 2007.

[4] K. Saito, R. J. Spence, C. Going, and M. Markus, "Using high-resolution satellite images for post-earthquake building damage assessment: A study following the 26 January 2001 Gujarat earthquake," *Earthquake Spectra*, vol. 20, no. 1, pp. 145–170, Feb. 2004.

[5] F. Yamazaki, Y. Yano, and M. Matsuoka, "Visual damage interpretation of buildings in Bam city using QuickBird images following the 2003 Bam, Iran, earthquake," *Earthquake Spectra*, vol. 21, no. S1, pp. 329–336, Dec. 2005.

[6] L. P. Lei, L. Y. Liu, L. Zhang, J. T. Bi, and Y. H. Wu, "Assessment and analysis of collapsing houses by aerial images in the Wenchuan earthquake," *J. Remote Sens.*, vol. 14, no. 2, pp. 333–344, May 2010.

[7] H. Mitomi, F. Yamazaki, and M. Matsuoka, "Development of automated extraction method for building damage area based on maximum likelihood classifier," in *Proc. 8th Int. Conf. Struct. Safety Reliab.*, 2001, p. 8,

[8] F. Yamazaki, D. Suzuki, and Y. Maruyama, "Detection of damages due to earthquakes using digital aerial images," in *Proc. 6th Int. Workshop Remote Sens. Disaster Appl.*, Pavia, Italy, 2008, [CD-ROM].

[9] D. C. Duro, S. E. Franklin, and M. G. Dubé, "A comparison of pixel-based and object-based image analysis with selected machine learning algorithms for the classification of agricultural landscapes using SPOT-5 HRG imagery," *Remote Sens. Environ.*, vol. 118, pp. 259–272, Mar. 2012.

[10] P. J. Li, H. Q. Xu, and J. C. Guo, "Urban building damage detection from very high resolution imagery using OCSVM and spatial features," *Int. J. Remote Sens.*, vol. 31, no. 13, pp. 3393–3409, Jul. 2009.

[11] M. Turker and B. Cetinkaya, "Automatic detection of earthquake-damaged buildings using DEMs created from pre- and post-earthquake stereo aerial photographs," *Int. J. Remote Sens.*, vol. 26, no. 4, pp. 823–832, Feb. 2005.

[12] X. H. Tong, Z. H. Hong, and S. J. Liu, "Building-damage detection using pre- and post-seismic high-resolution satellite stereo imagery: A case study of May 2008 Wenchuan earthquake," *ISPRS J. Photogramm. Remote Sens.*, vol. 68, no. 2, pp. 13–27, Mar. 2012.

[13] M. Turker and E. Sumer, "Building-based damage detection due to earthquake using the watershed segmentation of the post-event aerial images," *Int. J. Remote Sens.*, vol. 29, no. 11, pp. 3073–3089, Jun. 2008.

[14] X. H. Tong *et al.*, "Use of shadows for detection of earthquake induced collapsed buildings in high-resolution satellite imagery," *ISPRS J. Photogramm. Remote Sens.*, vol. 79, pp. 53–67, May 2013.

[15] C. Strecha and O. Küng, 2011. [Online]. Available: http://www.pix4d.com

[16] G. Grunthal, *European Macroseismic Scale 1998 (EMS-98)*. Luxembourg, U.K.: European Seismological Commission , 1998.

[17] P. A. Burrough and R. A. McDonell, *Principles of Geographical Information Systems*. New York, NY, USA: Oxford Univ. Press, 1998.

[18] Y. W. The, M. I. Jordan, M. J. Beal, and M. B. David, "Hierarchical Dirichlet processes," *J. Amer. Stat. Assoc.*, vol. 101, no. 476, pp. 1566– 1581, Dec. 2006.

[19] M. Y. Liu, O. Tuzel, S. Ramalingam, and R. Chellappa, "Entropy rate superpixel segmentation," in *Proc. IEEE Comput. Vis. Pattern Recog.*, 2011, pp. 2097–2104.

[20] I. O. Kyrgyzov, O. O. Kyrgyzov, H. Maître, and M. Campedel, "Kernel MDL to determine the number of clusters," in *Machine Learning and Data Mining in Pattern Recognition*. Berlin, Germany: Springer-Verlag, 2007, pp. 203–217.

[21] W. Yi, H. Tang, and Y. H. Chen, "An object-oriented semantic clustering algorithm for high-resolution remote sensing images using the aspect model," *IEEE Geosci. Remote Sens. Lett.*, vol. 8, no. 3, pp. 522–526, May 2011.

[22] H. Tang *et al.*, "A multiscale latent Dirichlet allocation model for object oriented clustering of VHR panchromatic satellite images," *IEEE Trans. Geosci. Remote Sens.*, vol. 51, no. 3, pp. 1680–1692, Mar. 2013.

[23] L. Shen *et al.*, "A semi-supervised latent Dirichlet allocation model for object-based classification of VHR panchromatic satellite images," *IEEE Geosci. Remote Sens. Lett.*, vol. 11, no. 4, pp. 863–867, Apr. 2014.

[24] A. Madabhushi, D. N. Metaxas, "Combining low-, high-level and empirical domain knowledge for automated segmentation of ultrasonic breast lesions," *IEEE Trans. Med. Imag.*, vol. 22, no. 2, pp. 155–169, Feb. 2003.

Author's Profile

Ms. Afra Fatima has completed B.TECH (ECE) from Shadan Women's College of Engineering And Technology, Khairthabad. JNTU University Hyderabad. Presently, she is pursuing her Masters in DIGITAL SYSTEM and COMPUTER Engineering from Shadan Women's College Of Engineering And Technology, Hyderabad, TS. India.

K. Premlatha has completed M.tech in ECE with specialization (Digital Systems and Computer Electronics) from JNTUH in 2005. She has completed B.E in EC.E from S.R.K.R Engineering College affiliated by Andhra University in 2000. Currently she is working as an Associate Professor in ECE Department at Shadan Women's College of Engineering & Technology, Hyderabad from 2005. Her areas of Research interest include Low Power VLSI, Digital Systems Design , Design for Testability.